

Favoured Local Structures in Liquids and Solids: a 3D Lattice Model

Pierre Ronceray

*Laboratoire de Physique Théorique et Modèles Statistiques,
Univ. Paris-Sud, Bât. 100, 91405 Orsay Cedex, France*

and Peter Harrowell

School of Chemistry, University of Sydney, Sydney N.S.W. 2006, Australia

We investigate the connection between the geometry of Favoured Local Structures (FLS) in liquids and the associated liquid and solid properties. We introduce a lattice spin model – the FLS model on a face-centered cubic lattice – where this geometry can be arbitrarily chosen among a discrete set of 115 possible FLS. We find crystalline groundstates for all choices of a single FLS. Sampling all possible FLS's, we identify the following trends: i) low symmetry FLS's produce larger crystal unit cells but not necessarily higher energy groundstates, ii) chiral FLS's exhibit to peculiarly poor packing properties, iii) accumulation of FLS's in supercooled liquids is linked to large crystal unit cells, and iv) low symmetry FLS's tend to find metastable structures on cooling.

I. INTRODUCTION

For a given interaction potential between particles, some local arrangements will be particularly stable and these *favoured local structures* (FLS) will thus accumulate in the liquid upon cooling. There is a considerable body of literature on the geometric and kinetic consequences of these FLS's in supercooled liquids, which have been the subject of a number of recent reviews [1, 2]. A possibility that has remained of perennial interest since first suggested by Frank in 1952 [3] is that if a single FLS dominates the liquid structure and its geometry is incompatible with crystalline symmetries, it could stabilize the liquid down to the point of dynamical arrest. This is the starting point of the *geometrical frustration* approach to understanding the glass transition [4]. The fundamental question of this field can be posed as follows: might there be favoured local structures of such geometrical awkwardness that they either do not have a periodic ground state or, if they do, it is so high in energy that the freezing point is forced down well below the limit of kinetic accessibility?

To properly address this question it is important that we consider the consequences of any particular set of FLS's for *both* the crystal phase as well as the liquid state. Indeed, the stability of the liquid depends crucially on the stability of the crystal and the kinetics of transformation into that ordered structure. In adopting this perspective, physical consistency requires that the crystal structure must be assembled out of the same set of FLS's available to the liquid. The fact that the simulation studies of liquid FLS's typically report little or no concentration of the crystalline local structure [1, 2] (despite their stability) is, we suggest, a consequence of the high symmetry of the local environments found in the small unit cell crystals frequently represented in simulation models. As we have previously shown [5], a liquid can only accommodate a low concentration of high symmetry FLS's due to their high entropy cost. In cases where the crystal unit cell is larger than just the nearest

neighbour coordination, the crystal local structure has been observed at high densities in the supercooled liquid [6].

Reports of systematic searches of low energy or high density crystal structures have appeared with increasing frequency in recent years [11]. These studies have highlighted the extraordinary variety of crystal structures that can be accessed by the parametrization of simple shapes. The role of local structure in liquids remains a more challenging question. The structure of molten salts has generated an extensive literature [12] as has the structures in liquids characterized by local tetrahedral order such as silica [13]. Even in cases when the local structures are complex and multiple, there exists a strong conviction that they represent an essential key to understanding the properties of the low temperature phases. A considerable body of work addresses the favoured local structures in binary and ternary atomic alloys [2]. These local structures have been associated with dynamic arrest and slow crystallization rates [2].

Our objective is to complete a systematic study of how changes in the geometry of the FLS influence the properties of the liquid and crystal phases. To carry this out through adjustments of the interparticle potential would be difficult, requiring the invention of a set of complex potentials for the task. In this article we shall circumvent this problem by explicitly defining our Hamiltonian in terms of the FLS's themselves. In this way we simply assign potential energies to each of the possible FLS's so as to favour selected local structures. As the number of possible FLS's can be large, even this simple recipe can generate an enormous number of possible Hamiltonians so we shall restrict our attention to the cases where only a single local structure at a time is favoured. With this restriction we shall not be able to directly address the original Frank picture [3, 4] which requires at least two FLS's - an icosahedral structure assumed to dominate the liquid structure and the cube octahedron that characterises the local structure of the face centred cubic (fcc) crystal. The influence of multiple FLS's we leave

for future work.

In this paper we implement this FLS Hamiltonian using Ising spins on the vertices of an fcc lattice. We have previously reported on the features of this FLS model in two dimensions, where we explored the relationship between the FLS and the crystal structure [7], liquid entropy [5], the freezing transition [8] and the role of chirality [9]. In this paper we shall examine how these various observations are influenced by the increase to 3D. The immediate challenge of the 3D FLS model is the significant increase in the number of possible FLS's - from 9 in 2D to 115 in 3D.

The paper is organised as follows. In Section II, we detail the definition of the three-dimensional model. We then turn to the description of the different regimes of interest: in Section III, we investigate the structural properties of the ground states, finding that they are all crystalline but can be very complex. In Section IV, we describe the thermal behaviour of the FLS model: liquid phase, supercooling and freezing transitions. Finally, Section V is devoted to an analytic study of the previously studied quantities, using statistical methods to connect structural and thermal properties. We discuss the consequences of our findings in Section VI. Details of the groundstate properties and transition behaviour for each FLS is provided as Supplementary Material [10].

II. THE MODEL

The Favoured Local Structures model is a model of Ising spins (*i.e.* binary variables) located at the vertices of a regular lattice. In this article we focus on the case of a three-dimensional face-centered cubic (fcc) lattice. The local structure at a given lattice site is defined as the spin conformation of the nearest neighbours of this site (regardless of the value of the spin at said site). Thus there are 2^z possible local structures at a given site, where $z = 12$ is the connectivity of the lattice. Among this large number of structures, some differ only by a rotation and are treated as indistinguishable, so that this model is isotropic. An instance of the model is obtained by selecting one local structure and making it *favoured* by directly stabilizing it. In order to do so, we attribute an energy of -1 to sites whose local environment corresponds to this *favoured local structure* (up to a rotation), while all other sites have zero energy. The total energy of a spin configuration is thus simply, up to a minus sign, the number of sites lying in the FLS. We consider configurations of such systems on a large lattice with periodic boundary conditions, in the canonical ensemble. The temperature thus controls the density of Favoured Local Structures, and the zero-temperature limit corresponds to dense packing of FLS on the lattice.

On the two-dimensional triangular lattice previously studied [5, 7–9], $z = 6$ and thus there were 64 possible local structures, falling into 14 rotationally distinct classes. As the model turns out to be the same when one FLS or

its spin inverted variant is selected, there were 9 possible choices left. Finally, two of these local structure were *chiral*, *i.e.* they lacked a reflection symmetry, and formed an *enantiomer pair*. While the model would be identical by selecting either of those enantiomers, we found interesting to distinguish the case when only a one of them is favoured – the *chiral* case – from that when both are favoured – the *racemic* case. Physically, the racemic case might correspond either to an equimolar mixture of enantiomers or to a flexible molecule with two enantiomeric conformations. This left us with 9 possible choices for the FLS, all of which were studied in detail.

In this article we consider the case of a face-centered cubic lattice, for which each site has $z = 12$ neighbours. The 4096 local structures reduce to 115 after removing those which are related by rotation or spin inversion of another. Among them, there are 39 enantiomer pairs for which we distinguish the racemic and the chiral cases, while the remaining 37 structures are achiral. A selection of these structures, where spins are represented by coloured spheres, is presented in the insets of Figure 1. All these structures are depicted, labelled and individually studied in the Supplementary Material [10]. We now report on the study of these 115 possible systems.

The main question we want to address is the influence of the local geometry on the macroscopic properties of the system. To quantify the degree of symmetry of the local structure, we introduce the size \mathcal{S} of the spatial point group of an FLS. This number ranges from $\mathcal{S} = 1$ for those FLS's with no symmetry save the identity operation to $\mathcal{S} = 48$, the size of the complete symmetry group of the lattice. The latter is attained only by one FLS, the all-up environment labelled $\mathbf{0}$, corresponding to ferromagnetic ordering. The inclusion of the racemic mixtures complicates the test for the influence of \mathcal{S} , since the added flexibility due to favouring two distinct enantiomers is not reflected by this symmetry parameter. Besides, we show in Section VB that the chiral symmetry is peculiar in our model. For these reason, we distinguish the sets of achiral, chiral and racemic FLS throughout the paper.

III. STRUCTURAL PROPERTIES AND GROUND STATES

In this Section, we present the ground state properties of the model, corresponding to dense packing of the FLS on the lattice.

A. Ground state energies

The ground state energies E_o , corresponding to minus the maximum packing density of the FLS, have been determined for all choices of FLS. These energies and the associated crystalline structures were determined by an enumerative process similar to that introduced by Hart

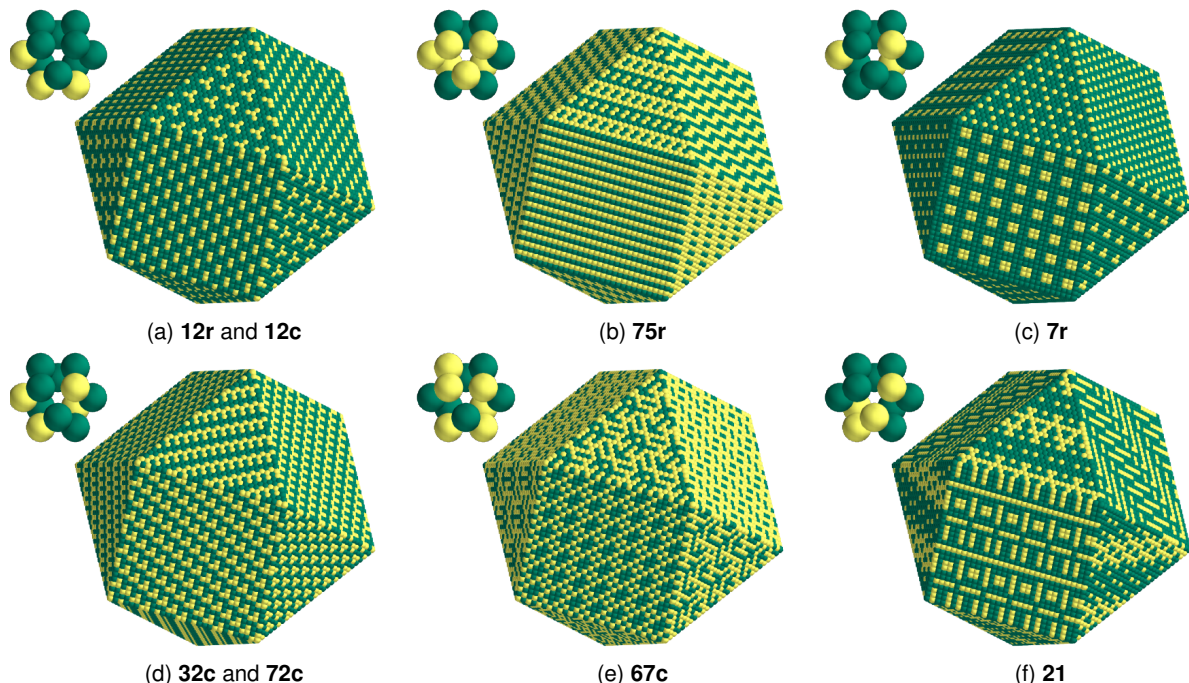


FIG. 1: A selection of ground state structures for various choices of the favoured local structure. This representation shows a portion of an infinite crystal, cut along different planes. The associated FLS is depicted in inset, while the labels correspond to those employed in Supplementary Material. For chiral FLS's, the letters **c** and **r** respectively correspond to systems with one and both enantiomers favoured.

and Forcade [15], detailed in the Appendix. *We found no evidence of a non-crystalline structure more stable than the crystals identified by this method.* A selection of crystalline structures is presented in Figure 1. A complete presentation of these structures is provided in ref. [10].

The distribution of ground state energies is plotted in Figure 2. These energies are integer fractions, corresponding to minus the ratio of the number of FLS in the crystal cell to the size Z of this crystal. The ground state energies range from -1 (corresponding to all sites in the FLS, attained by three local structures) to $-1/4$, the lowest packing fraction obtained (attained by five chiral FLS's). Notably, chiral FLS's tend to have higher ground state energy than other structures, a fact that will be discussed in Section V B. There is a particularly large peak at $E_o = -1/2$ characterized mostly by structures consist of an alternating 2D layers that are either completely filled or completely empty of FLS.

With an average of $\langle E_o \rangle = -0.51(0.17)$ [30], the minimal energies are generally considerably higher than those observed in 2D [7], for which $\langle E_o \rangle = -0.73(0.13)$. This effect of dimension is analogous to the well documented decrease in maximum packing density for hard spheres with increasing dimensionality [16]. The increase in the number of nearest neighbour sites resulting from an increase in spatial dimension appears to generate more constraints with regards to packing than it provides degrees of freedom to resolve them, giving rise to the observed

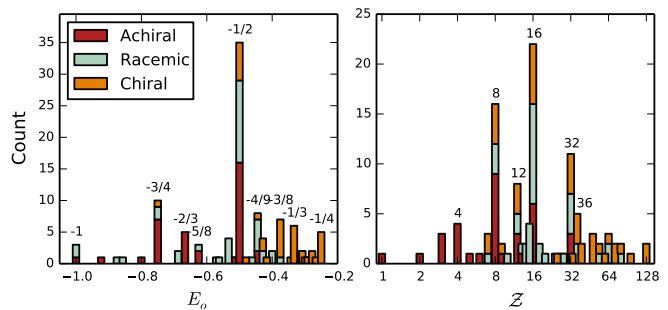


FIG. 2: The distribution of ground state energies E_o (left panel) and crystal cell size (right panel). The colors indicate the nature of the FLS.

decrease in packing density.

All but one of the racemic groundstates, for which both enantiomers are equally favoured, consist of actually racemic crystals with equal numbers of each enantiomer. This outcome is not imposed by the Hamiltonian, as evidenced by the one exception, the racemic FLS **12r**, whose groundstate contains only a single enantiomer, resulting in a crystal structure identical to that of the chiral option **12c**. This crystal is depicted in Figure 1(a). In the case of chiral organic molecules, there is considerable interest in understanding the conditions under which crystallization might select a single enantiomer from a racemic mixture.

Starting with Pasteur’s famous separation of the enantiomers of tartaric acid [19], enantiomer-selective crystallization represents an important route to obtaining single enantiomer populations of molecules. Empirically, chiral organic molecules are found to crystallize preferentially into the pure enantiomer in 10% of cases [20]. Our one example, the FLS **12r**, is insufficient to establish any general rule. That said, we note the groundstate energy of the chiral crystal **12c**, $E_o = -3/4$, is only case of a chiral crystal with an energy lower than $-1/2$.

Our FLS model clearly demonstrates that the racemic crystal is generally more stable than its chiral counterpart. This stability is highlighted by the fact that, of the three choices of FLS which achieve perfect packing, *i.e.* $E_o = -1$, two are racemic; **74r** and **75r** (see Figure 1(b) for the structure of the latter case). These perfect packings, along with the general trend for enantiomers to pack in equal proportion point to a general packing benefit that is afforded low symmetry FLS’s when they can be paired with their enantiomer. The resulting dimer has a higher symmetry (gaining, at the least, a centre of inversion) and this allows for a greater number of crystal types to be considered which, in turn, would be expected to lead to a lower groundstate energy.

B. Crystalline cell sizes

The unit cell size \mathcal{Z} of the groundstate crystal structure provides some measure of the structural complexity of the crystal since the larger \mathcal{Z} , the number of lattice sites within the unit cell, the greater the information required to specify the structure. In Figure 2 we plot the distribution of unit cell sizes, revealing a large variation, ranging from 1 to 128, with peaks at powers of 2. A selection of crystalline ground state structures is presented in Figure 1.

The size of the largest unit cells observed in the FLS model is of particular interest. On a practical point, a unit cell of 128 sites highlights the difficulty of ensuring that the simulation volume is appropriately shaped to accommodate the crystal. The occurrence of crystals with large unit cells is also a topic of considerable physical interest. Pauling, in 1955, solved the structure of an intermetallic alloys, NaCd_2 , to find that the unit cell was huge, containing 1152 atoms [21]. Since this pioneering result, intermetallic alloys have provided a growing number of what have been labelled *giant unit cell* structures [22], with hundreds of cases of cells whose size exceeds 10^3 atoms. The study of such giant unit cell structures has been identified [22] as “one of the last white spots on the map of metal physics”. At issue are the twin problems of the description of their organization and of the identification of the mechanism by which they are formed from the liquid state.

We find two chiral FLS’s, **28c** and **67c**, which exhibit groundstates with a cell size $\mathcal{Z} = 128$. The groundstate of the the FLS **67c** is shown in Figure 1(e). Despite

this apparent structural complexity, we find both crystals nucleate and grow spontaneously in Monte-Carlo simulated annealing of sufficiently large systems, confirming that they are indeed kinetically accessible from the supercooled liquid. A preliminary examination of the crystal structures of the **28c** and **67c** groundstates indicate the presence of asymmetric unit cells, $8 \times 4 \times 4$ and $8 \times 8 \times 2$ respectively, characterised by repeated motifs of clusters of FLS’s. Unravelling the energetics and kinetics of assembly of such hierarchical structures remains an interesting challenge.

IV. THERMAL PROPERTIES

We now turn to the study of the FLS model at finite temperature in the canonical ensemble. We first present the properties of the equilibrium liquids and the equilibrium freezing transitions. We then move to the non-equilibrium properties, by investigating the dynamics in the supercooled liquid and the low-temperature fate of an annealed system.

A. Equilibrium liquids and freezing transitions

Top panels of Figure 3 present the temperature dependence of the average energy (*i.e.*, minus the FLS density) in canonical ensemble simulations of the model, for various choices of the FLS. A striking feature of these curves is the strongly first-order nature of the freezing transitions, which is generic of the model. In an hysteresis cycle, we observe both strongly supercooled liquid and overheated crystal. In order to locate the *equilibrium* freezing point, we employed a Maxwell construction, as in the 2D model [8]. The resulting temperature is indicated as a thick red vertical line in Figure 3.

1. Order and its Entropy Cost in the Liquids

At infinite temperature, the liquid has a finite energy which we denote E_∞ , due to random appearances of the local structure in a completely disordered spin system. These infinite temperature FLS densities do not exceed 0.012. We can evaluate the ordering of the liquid by relating its FLS density to the asymptotic regimes $T = 0$ and $T = \infty$. We introduce the order parameter ϕ , defined as [7]

$$\phi(T) = (E(T) - E_\infty)/(E_o - E_\infty) \quad (1)$$

In Figure 4, we present the distribution of the maximum value of ϕ attained in the equilibrium liquid (*i.e.* the value at the freezing point T_f). We find that it is very small in most cases, with an average of $\langle \phi(T_f) \rangle = 0.11(0.1)$, indicating negligible ordering in the liquid. It is less than 0.1 in 71 cases out of 115, and more than 0.3

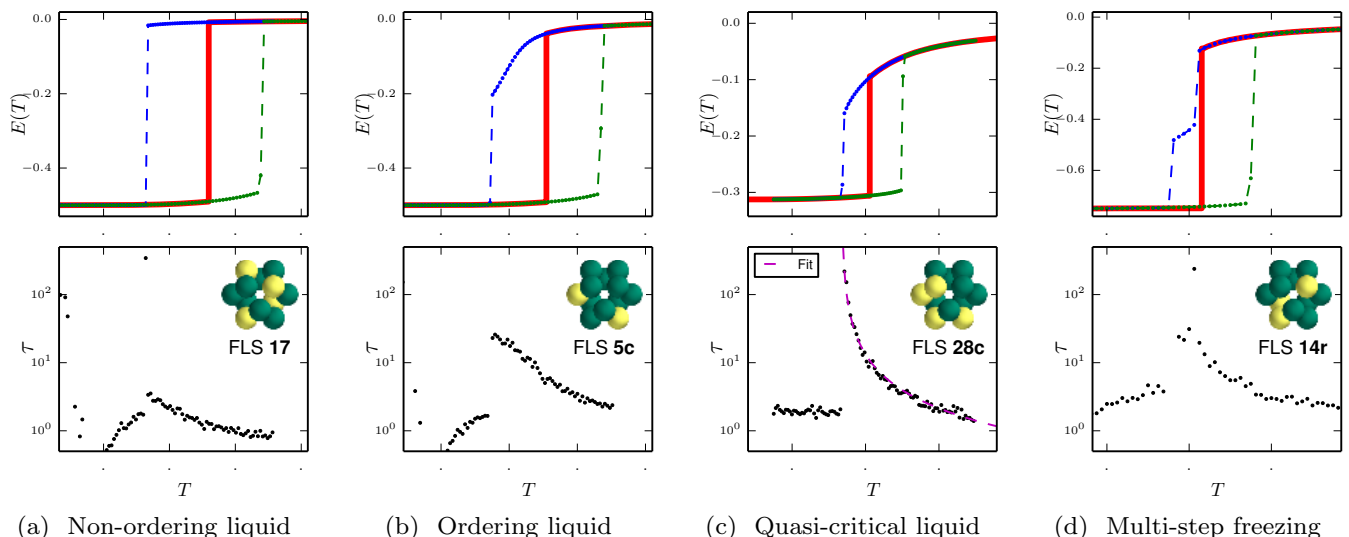


FIG. 3: Top row: The energy *versus* temperature curves for a selection of FLS's. Monte-Carlo simulations of an hysteresis cycle are shown in blue and green dots (respectively cooling and heating), with the dashed line indicating freezing and melting transitions. The thick red curve corresponds to a thermodynamic calculation of the equilibrium curve by a Maxwell construction. Bottom row: the energy autocorrelation time, in log-scale.

in only five cases. This is in sharp contrast with the 2D model, for which equilibrium liquids with $\phi(T_f) > 0.8$ were observed.

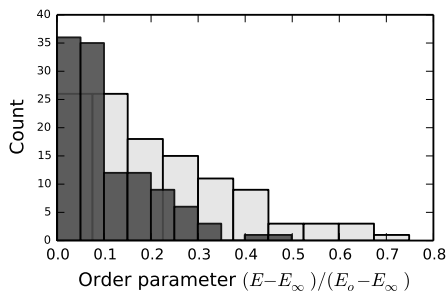


FIG. 4: Statistics for the amount of ordering. Dark gray: at the equilibrium crystallization transition, and light gray: at the limit of stability of the supercooled liquid.

The energetic gain of increasing the density of favoured local structures competes, at finite temperature, with the entropy loss associated to this increased order. This entropy cost can be assessed by performing a high temperature expansion of the energy-entropy relation, as already discussed in the 2D case [5],

$$S = S_\infty - \frac{A}{2}(E_\infty - E)^2 + O((E_\infty - E)^3) \quad (2)$$

where $S_\infty = \ln(2)$ (the maximum entropy of a binary spins system), and A is the entropy cost parameter quantifying the decrease in entropy with decreasing energy. The larger the value of A , the more rapidly the liquid

loses entropy as the density of FLS's increases and the higher the temperature at which the liquid becomes thermodynamically unstable with respect to the solid. We established in [8] that this high temperature expansion is actually a cluster expansion, where the coefficient A is related to the statistics of pairwise overlaps between neighbouring FLS's. We calculated the values of A for the 3D FLS model and find them to be of the order of 150, considerably larger than the analogous values for the 2D model (which are of the order of 5). Thus the entropy cost for a specific FLS in 3D is considerably higher than that found in 2D. This result is due to the much larger number of local structural possibilities in 3D as compared to 2D and, hence, the greater entropy loss when a single FLS is selected.

This high entropy cost places a serious limit on the density of FLS's the liquid state can physically accumulate. Kauzmann [23] noted that extrapolations of the liquid entropy to low temperatures suggested that the entropy would vanish at some non-zero temperature. Equation 2 implies an analogous disappearance of the liquid entropy (and, hence, the 'end' of any liquid state) at an energy E_K , related to A by

$$E_K = E_\infty - \sqrt{\frac{2S_\infty}{A}} \quad (3)$$

Based on this, admittedly simplistic, estimate, the values of E_K range between -0.16 and -0.02 , underlining the very limited amount of structure the 3D FLS liquids can accumulate. As discussed below, some of the supercooled liquids in the FSL model achieve energies much lower than -0.16 indicating the limits of this high-temperature

estimate, which neglects cooperative effects of more than 2 FLS.

2. Equilibrium Freezing Temperatures

Given the low densities of the FLS in the equilibrium liquid, it is reasonable to approximate the liquid with its high temperature limit. Likewise, the crystal shows little decrease in order prior to melting, as shown in Figure 3. Neglecting order in the liquid and loss of order in the crystal, we obtain an approximate formula for freezing temperatures:

$$T_f \approx \frac{|E_o|}{\ln 2} \quad (4)$$

This expression depends solely on the ground state energy, with no dependency on the liquid properties. In Figure 5, we plot the freezing temperatures obtained by Maxwell construction against the ground state energies and compare them with the approximate expression of Equation 4. The data for the 2D model are also shown in the same graph. We find that Equation 4 provides excellent agreement with the values of the freezing temperature for the FLS model on the FCC lattice. This success is in stark contrast to the 2D case where the theoretical expression substantially overestimates T_f .

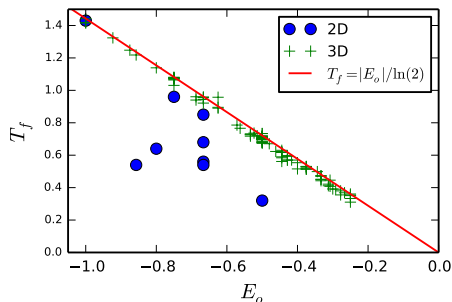


FIG. 5: The freezing temperature T_f against the ground state energy E_o , for both the 3D (crosses) and the 2D (circles) FLS model. The line corresponds to theoretical Equation 4.

B. Supercooling the Liquid

Many of the FLS's result in liquids that exhibit a marked supercooling before freezing. In this Section and the next, we employ a standard cooling rate of 5.10^6 rejection-free MC steps per site and per unit of temperature, for system sizes of order 24^3 .

1. General Characteristics of the Supercooled Liquid

We find that the average ratio of the minimum temperature T_{\min} to which the liquid can be cooled to that of the freezing point to be $\langle T_{\min}/T_f \rangle = 0.79(0.09)$. This supercooling is significant and considerably larger than observed in the 2D model [8], apart from the one chiral case [9]. In molecular liquids, the glass transition T_g is typically associated with a deeper supercooling, i.e. T_g/T_f 0.66 [24].

Supercooling is associated with an increase in the density of FLS above that observed at coexistence. In Figure 4, we report the distribution of ϕ calculated at the lowest value of the temperature to which each liquid can be supercooled. Here we find a handful of liquids reaching over half of the order of the groundstate crystal. The average is $\langle \phi(T_{\min}) \rangle = 0.21(0.17)$, twice that at the equilibrium crystallization transition.

2. Supercooling Scenarios

In Figure 3 we plot the average energy $E(T)$ and the energy autocorrelation time $\tau(T)$ (measured in Monte-Carlo steps per site), estimated by the method of batch means [25] as a function of T . We have distinguished several different scenarios based on the behaviour of the temperature dependence of E and τ in the supercooled regime. Examples of each scenario are presented. The properties of each scenario are described as follows.

i) *Non-Ordering Liquid* (79 FLS's). The most common scenario in this model is characterized by a liquid showing negligible cooperativity down to the freezing transition, as illustrated on Figure 3a. Even at the lowest temperature T_{\min} at which the metastable liquid can be observed, the energy autocorrelation time remains small, only 3.5 MC steps per site.

ii) *Ordering Liquid* (22 FLS's). The cases not included within the 'Non-Ordering' category exhibit a significant accumulation of FLS. Figure 3b is a good example of this scenario. While the *equilibrium* liquid exhibits almost no ordering ($\phi(T_f) = 0.07$), the supercooled liquid is characterized by a steady accumulation of FLS, with a high and approximately constant heat capacity $C_v = \partial E/\partial T$. In this regime, the dynamical time scale grows steadily up to $\tau \approx 30$ MC steps per site, indicating the existence of cooperative effects in the supercooled liquid.

iii) *Quasi-Critical Liquid* (14 FLS's). In a number of cases, the relaxation time τ is strongly non-Arrhenius and can climb up to 10^3 MC steps per site (our limit of time resolution for τ), exhibiting an apparent divergence at the end of the supercooled branch, with a correspondingly strong increase in heat capacity. This behaviour is illustrated on Figure 3c. The autocorrelation time is well fitted by a diverging power law $\tau \propto |T - T_c|^{-\gamma}$ with an exponent $\gamma \approx 1.3$ (dashed line in Figure 3c). While this scenario resembles that of a glass transition, we note that this supercooled branch terminates with a discontinuous

transition in the energy in all cases in this model.

C. Low Temperature States Following Quenching

While we always observe a discontinuity in energy at the freezing transition when annealing the system, the resulting low-temperature state varies and the ground state crystal is not always obtained. We now discuss the different classes of $T = 0$ structure observed following a quenching via Monte Carlo dynamics.

i) *Standard Crystallization* (99 FLS) The most common scenario corresponds to the formation of a crystal structurally similar to the ground state computed from the enumerative method. There is some variability between cases in this family. For 66 FLS's, the observed state corresponds exactly to the computed ground state, provided that the boundary conditions were adapted to the crystal structure. In 9 FLS's, we find the predicted groundstate crystal is formed but as polycrystalline, with domains separated by grain boundaries, as illustrated in Figure 6a. In a rather large number of cases (24 FLS's), the system cooperatively orders into a state with the same energy as the calculated ground state, but with apparent degrees of freedom remaining. We tentatively qualified these states as “plastic”, without intending to assert any specific connection with the more clearly defined plastic crystal phases of molecular systems [27]. This is reminiscent of the ground state structure of the antiferromagnetic Ising model on a triangular lattice, for which frustration effects lead to a highly degenerate ground state. Finally, we observe 3 FLS's to crystallize into the predicted groundstate but via an intermediate mesophase whose stability remains unclear. An example of this multi-step crystallization is illustrated in Figure 3d. Note that the mesophase is observed only on cooling of the liquid, and at temperatures lower than the computed equilibrium transition between liquid and crystal.

We also identified two scenarios for which the low-temperature state was structurally and energetically different from the predicted ground state.

ii) *Metastable Polymorph Formation* (14 FLS) In these cases, a recognizably crystalline structure was consistently obtained, albeit with an energy strictly higher than the ground state. This scenario is illustrated in Figure 6b, for which a complex crystalline state with energy $-4/9$ and a huge cell size $Z \geq 288$ was obtained, while a much simpler and stabler crystalline structure with energy $-1/2$ and cell size $Z = 16$ was available. In some cases the crystal state formed can vary between different cooling runs. This is clear evidence of polymorphism. We do not know, in each case, whether the higher energy structure is, in fact, a true equilibrium phase at the freezing temperature, favoured over the lower energy structure by entropic effects, or a metastable crystal, selected by the kinetics of ordering. The demonstration that our model includes polymorphs is interesting given

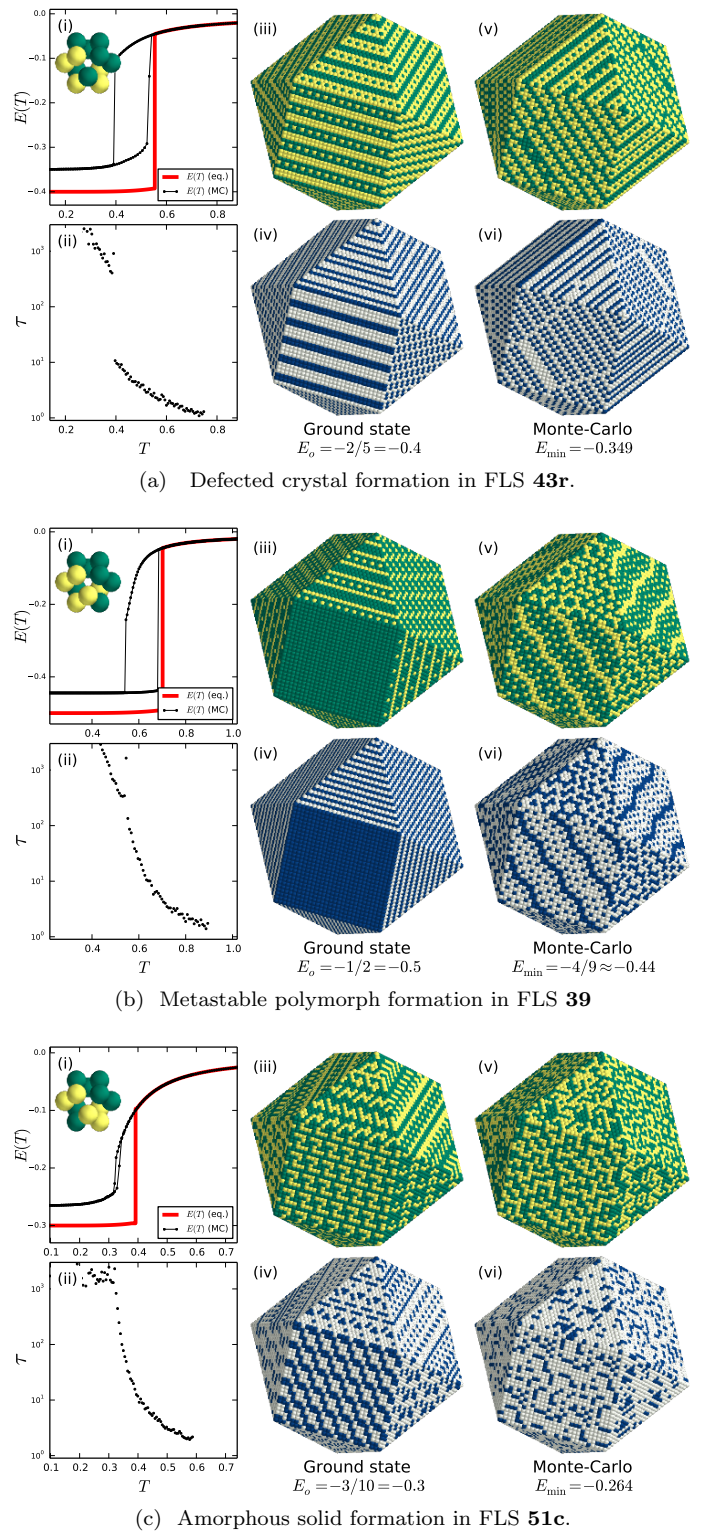


FIG. 6: Three scenarios for avoided crystallization. In each case, we display: (i) the $E(T)$ curve with a picture of the FLS in inset and (ii) the energy autocorrelation time $\tau(T)$, as in Fig. 3; (iii) the computed crystalline structure and (v) a low-temperature state from Monte-Carlo simulations; (iv) and (vi) the respective associated location of the favoured local structures (FLS sites in blue, non-FLS in white).

the prevalence of polymorphs in molecular crystals. In one well studied case [26], a molecule has been observed to crystallize into 7 distinct crystal structures.

iii) *Amorphous Solid Formation* Finally, in a single case, the FLS **51c**, the liquid freezes with an apparent discontinuity of the energy into an amorphous state with no recognizable trace of crystallinity (see Figure 6c). This transition is accompanied by a dynamical arrest of the supercooled liquid, in the quasi-critical scenario discussed in Section IV B, and the relaxation time scale becomes larger than our resolution of $\tau = 10^3$ MC steps per site. On heating this state, negligible hysteresis is observed. It is not clear whether this puzzling behaviour corresponds to a conventional glass transition (for which the energy would have to be continuous) or some sort of polycrystalline aggregation. What is clear is that the **51c** case represents the interesting possibility of the formation of an amorphous solid stabilized entirely (by construction) by the same FLS as stabilizes the crystal.

V. ON THE CORRELATION BETWEEN THE FLS STRUCTURE AND THE PROPERTIES OF THE LIQUID AND SOLIDS STATES

In the previous sections, we have described the variety of behaviours of our model, going through different aspects of its macroscopic properties: crystalline ground states, liquids and supercooled liquids, freezing transitions and low-temperature states. In this Section, we examine a number of hypotheses associated with how the choice of FLS determines the collective properties of the system. A summary of our conclusions and the statistical data on which they are based is presented in Table I.

A. Structure of the Ground State

We start by considering the influence of the symmetry properties of the FLS (the size \mathcal{S} of the spatial point group of an FLS introduced in Section II) on the structure of the ground state. In Section III we introduced two observables to quantify the latter: the ground state energy E_o measures the quality of the packing, while the cell size \mathcal{Z} measures its complexity. We disentangle the correlations between these quantities by restricting the statistical analysis to sets of FLS for which one parameter is fixed – for instance, we analyze the correlation between \mathcal{S} and E_o by considering the 22 FLS’s with crystal cell $\mathcal{Z} = 16$. This is made possible by the existence of sharp peaks in the histograms of Figures 2. Because \mathcal{Z} and \mathcal{S} vary over several orders of magnitude, we consider their logarithm when measuring correlations.

The connection between symmetry and ground state energy is investigated in Table Ia. There appears to be no significant correlation between E_o and \mathcal{S} : the degree of symmetry of the local structure does not influence its ground state energy. This is perhaps surprising, as one

might expect awkward objects of low symmetry to have poor packing properties. We interpret the independence between E_o and \mathcal{S} as the compensation of two effects: on the one hand, high-symmetry objects are more likely to fit well together; on the other hand, low-symmetry objects have more rotational variants, thus offering a wider pool of combinations to select the ground state from.

On the other hand, \mathcal{S} and \mathcal{Z} are significantly correlated, with a correlation ratio $r = -0.64$, as reported in Table Ib. Thus the cell size increases with decreasing symmetry. However, this trend is loose and admits exceptions: for instance, highly symmetric FLS **7r**, for which $\mathcal{S} = 6$, has a large unit cell $\mathcal{Z} = 64$ depicted in Figure 1(c). On the other hand, low-symmetry FLS **32c** (with $\mathcal{S} = 1$) crystallizes in a simple structure with $\mathcal{Z} = 7$, as depicted in Figure 1(d).

B. The special role of the chiral symmetry

As already hinted in Section III A, the ground state energies of chiral FLS are generally higher than those of achiral structures. This claim is properly confirmed in Table Ic, by comparing two groups of FLS with identical degree of symmetry: on the one hand the 19 achiral FLS’s with a plane reflection symmetry only, and on the other hand the 10 chiral FLS’s with only a rotational symmetry of order 2. We observe a statistically significant difference in the average ground state energy, while the difference in crystal cell size is insignificant. This shows that plane reflection symmetry of the structure plays a special role in determining the ground state energy: chiral local structures pack less densely than achiral structures. This special role of the chiral symmetry in such discrete packing problems is, to our knowledge, an original result of this study.

C. Crystallization or not?

We next turn to the question of the influence of structural properties on the low temperature fate of the system. We consider on the one hand the 90 “crystallizers” which find their exact ground state, and on the other the 16 FLS’s which do not find their ground state structure, and form either a glassy state or a metastable polymorph. We exclude defected crystals from this analysis, as they lie in-between. The dominant contribution is the symmetry factor: low symmetry strongly conditions towards avoided crystallization, as demonstrated in Table Id.

Because low symmetry structures also tend to form large crystal cells (Table Ib), crystal formation also strongly correlates with crystal cell size. However, we can refine this observation by considering the set of FLS with $\mathcal{S} = 1$. In Table Ie, we show that the value of \mathcal{Z} does not significantly affect the probability to fail crystallization within this population. To conclude, we have found that low symmetry FLS tend to crystallize less

TABLE I: Summary of our correlation hypotheses and associated conclusions. Their validity is assessed by the p -value, corresponding to the likelihood of observing comparable correlations in the case of independent variables, as provided by either Pearson’s analysis* or Student’s t -test†. Numbers in parentheses are standard deviations.

Question	Method employed and results	Conclusion															
(a) Does the symmetry of the FLS affect the ground state energy?	Compare E_o and $\log \mathcal{S}$ at fixed \mathcal{Z} <table border="1"> <thead> <tr> <th>Data set</th> <th># points</th> <th>Pearson r</th> <th>p-value*</th> </tr> </thead> <tbody> <tr> <td>$\mathcal{Z} = 16$</td> <td>22</td> <td>0.015</td> <td>0.95</td> </tr> </tbody> </table>	Data set	# points	Pearson r	p -value*	$\mathcal{Z} = 16$	22	0.015	0.95	No, they are uncorrelated.							
Data set	# points	Pearson r	p -value*														
$\mathcal{Z} = 16$	22	0.015	0.95														
(b) Does the symmetry of the FLS affect the crystal structure?	Compare $\log \mathcal{Z}$ and $\log \mathcal{S}$ at fixed E_o . <table border="1"> <thead> <tr> <th>Data set</th> <th># points</th> <th>Pearson r</th> <th>p-value*</th> </tr> </thead> <tbody> <tr> <td>$E_o = -1/2$</td> <td>35</td> <td>-0.64</td> <td>10^{-5}</td> </tr> </tbody> </table>	Data set	# points	Pearson r	p -value*	$E_o = -1/2$	35	-0.64	10^{-5}	Yes, \mathcal{Z} increases as \mathcal{S} decreases.							
Data set	# points	Pearson r	p -value*														
$E_o = -1/2$	35	-0.64	10^{-5}														
(c) Does chirality of the FLS influence the ground state energy?	Compare E_o for chiral and achiral populations. <table border="1"> <thead> <tr> <th>Data set</th> <th># points</th> <th>$\langle E_o \rangle$</th> <th>p-value†</th> </tr> </thead> <tbody> <tr> <td>Achiral, $\mathcal{S} = 2$</td> <td>19</td> <td>-0.55 (0.10)</td> <td>0.003</td> </tr> <tr> <td>Chiral, $\mathcal{S} = 2$</td> <td>10</td> <td>-0.41 (0.14)</td> <td></td> </tr> </tbody> </table>	Data set	# points	$\langle E_o \rangle$	p -value†	Achiral, $\mathcal{S} = 2$	19	-0.55 (0.10)	0.003	Chiral, $\mathcal{S} = 2$	10	-0.41 (0.14)		Yes, chiral FLS have a higher E_o than achiral ones.			
Data set	# points	$\langle E_o \rangle$	p -value†														
Achiral, $\mathcal{S} = 2$	19	-0.55 (0.10)	0.003														
Chiral, $\mathcal{S} = 2$	10	-0.41 (0.14)															
(d) Does the symmetry of the FLS affect the likelihood to form the ground state crystal?	Correlate low temperature state to symmetry \mathcal{S} . <table border="1"> <thead> <tr> <th>Data set</th> <th># points</th> <th>$\langle \mathcal{S} \rangle$</th> <th>$p$-value†</th> </tr> </thead> <tbody> <tr> <td>Crystallizing FLS</td> <td>90</td> <td>3.0 (5.3)</td> <td>0.007</td> </tr> <tr> <td>Avoided crystallization</td> <td>16</td> <td>1.25 (0.4)</td> <td></td> </tr> </tbody> </table>	Data set	# points	$\langle \mathcal{S} \rangle$	p -value†	Crystallizing FLS	90	3.0 (5.3)	0.007	Avoided crystallization	16	1.25 (0.4)		Yes, low symmetry FLS’s are more likely to avoid the groundstate.			
Data set	# points	$\langle \mathcal{S} \rangle$	p -value†														
Crystallizing FLS	90	3.0 (5.3)	0.007														
Avoided crystallization	16	1.25 (0.4)															
(e) Does the crystal cell size further affect the likelihood to fail crystallization?	Correlate low- T state to \mathcal{Z} at fixed symmetry \mathcal{S} . <table border="1"> <thead> <tr> <th>Data set</th> <th># points</th> <th>$\langle \mathcal{Z} \rangle$</th> <th>$p$-value†</th> </tr> </thead> <tbody> <tr> <td>Crystallizing FLS, $\mathcal{S} = 1$</td> <td>34</td> <td>31 (27)</td> <td>0.2</td> </tr> <tr> <td>Avoided cryst., $\mathcal{S} = 1$</td> <td>12</td> <td>38 (22)</td> <td></td> </tr> </tbody> </table>	Data set	# points	$\langle \mathcal{Z} \rangle$	p -value†	Crystallizing FLS, $\mathcal{S} = 1$	34	31 (27)	0.2	Avoided cryst., $\mathcal{S} = 1$	12	38 (22)		No, \mathcal{Z} does not influence crystallization at fixed \mathcal{S} .			
Data set	# points	$\langle \mathcal{Z} \rangle$	p -value†														
Crystallizing FLS, $\mathcal{S} = 1$	34	31 (27)	0.2														
Avoided cryst., $\mathcal{S} = 1$	12	38 (22)															
(f) Is there a link between the supercooling scenario and the groundstate properties?	Correlate the supercooling scenario to \mathcal{Z} and E_o . <table border="1"> <thead> <tr> <th></th> <th>Non-ordering</th> <th>Ordering</th> <th>Quasi-critical</th> <th>p-val.*</th> </tr> </thead> <tbody> <tr> <td>$\langle E_o \rangle$</td> <td>-0.56 (0.17)</td> <td>-0.42 (0.12)</td> <td>-0.36 (0.08)</td> <td>10^{-6}</td> </tr> <tr> <td>$\langle \mathcal{Z} \rangle$</td> <td>18 (18)</td> <td>32 (21)</td> <td>50 (32)</td> <td>10^{-7}</td> </tr> </tbody> </table>		Non-ordering	Ordering	Quasi-critical	p -val.*	$\langle E_o \rangle$	-0.56 (0.17)	-0.42 (0.12)	-0.36 (0.08)	10^{-6}	$\langle \mathcal{Z} \rangle$	18 (18)	32 (21)	50 (32)	10^{-7}	Yes, the supercooling scenario is linked to \mathcal{Z} and E_o (see discussion).
	Non-ordering	Ordering	Quasi-critical	p -val.*													
$\langle E_o \rangle$	-0.56 (0.17)	-0.42 (0.12)	-0.36 (0.08)	10^{-6}													
$\langle \mathcal{Z} \rangle$	18 (18)	32 (21)	50 (32)	10^{-7}													

than high symmetry ones, but that the crystal cell size – and hence its “complexity” – is no further impediment to crystallization. We note in particular that our three “giant unit cell” crystals with cell size $\mathcal{Z} > 80$ straightforwardly freeze into a perfect crystalline structure. On the other hand a low ground state energy favours crystallization. The latter observation can be intuitively explained by noting that a crystalline structure that is a deep minimum of energy – with low E_o – is less likely to have viable competing polymorphs than a high energy ground state.

Only a single FLS leads to an amorphous solid, as discussed in Section IV C, and we cannot make general statements on this basis. We note however that it is chiral, with minimal symmetry $\mathcal{S} = 1$, has a high ground state energy $E_o = -3/10$, and a large crystal cell $\mathcal{Z} = 80$. Variants or extensions of the present model could provide a larger population of similar amorphous systems, and give a statistical basis to draw more general trends.

D. Supercooling and ground state structure

The last point of our statistical analysis concerns the physical properties of the supercooled liquid and its connection with structural properties. In Section IV B, we qualitatively distinguished three different behaviours in the supercooled liquid: no trace of ordering, significant

ordering, and divergent time scale (“quasi-critical”). In Table I if we correlate this classification with the ground state energies and crystal cell sizes of all FLS’s.

We observe a clear trend: high order in supercooled liquids correlates with high ground state energy and large crystal cells. The first observation is not surprising. Indeed, as we have seen in Section IV A, high ground state energy correspond to low freezing temperatures, and thus to the possibility for the liquid to overcome high entropic barriers to ordering. On the other hand, the fact that crystal structure correlates with liquid ordering is rather unexpected, as in a simple nucleation picture the liquid does not “know” about the crystal structure. This is not a symmetry effect: restricting to the 26 chiral structures with $\mathcal{S} = 1$, we observe the same effect (although not resolved statistically).

VI. DISCUSSION

What are the macroscopic consequences of local structure in liquids? In this article, we addressed this question in the case when the favoured local structures found in the liquid and in the solid are the same – that is, when the ground state corresponds to a dense accumulation of a single FLS. We introduced a simple three-dimensional lattice model in which the FLS is explicitly specified. This Favoured Local Structures model on a 3D

face-centered cubic lattice provides a discrete set of 115 such structures to choose from, and we reported here on the comprehensive study of these systems. This large library of structures is a unique feature of this work and allowed us to employ an original statistical approach to correlate observable features of the model and unfold underlying physical laws. Given the similarity between different instances of the model – only the geometry of the FLS varies – the variety of observed behaviours is noteworthy.

We focused on the structural properties of the ground states – studying the relation between the symmetry of an FLS and its packing properties – and on the properties of the supercooled liquid – addressing the questions of how much order can be accumulated prior to freezing, and what solid phase will be formed at the freezing transition. Our main results can be summarized as follows:

1. All ground states are crystalline, with high variability in both the ground state energy $-1 \leq E_o \leq -1/4$ and unit cell size $1 \leq \mathcal{Z} \leq 128$. This structural complexity does not appear to present any systematic kinetic obstacle to crystallization.
2. We found no evidence that low symmetry FLS's result in 'poor' (*i.e.* high energy) crystals. Instead, we found that low symmetry FLS's tend to produce more complex crystals as characterised by larger unit cells. We interpreted this as resulting from compensating effects: low symmetry objects offer more orientational freedom than high symmetry ones, but the latter generally fit better together. We observed an exception to this rule in the case of chiral structures, which pack poorly, compared to achiral structures with equal degree of symmetry.
3. We observed only a single case of enantiomeric separation of a racemic mixture by crystallization. This exception corresponding to a chiral FLS that managed a particularly low energy groundstate.
4. The entropic cost of ordering in the liquid is so high in our model that we observe little organization prior to equilibrium crystallization. We regard this a consequence of the very strict definition of local structures in our model. Considering incomplete or multiple FLS could allow for more complex liquid behaviour.
5. Freezing transitions are typically strongly first-order and most liquids can be readily supercooled. Approaching the freezing transition, some liquids exhibit significant ordering and even apparently diverging relaxation times, while others remain unstructured. High ground state energy depresses the transition point towards low temperatures, allowing higher order in the liquid. More surprising, we found that systems whose crystalline structure is complex (*i.e.* large \mathcal{Z}) exhibit stronger ordering in the supercooled liquid, showing a significant correlation between the ground state structure and the amount of order in the amorphous state.
6. Finally, we found that low symmetry and high ground state energy FLS tend to avoid crystallization by either falling into a metastable crystalline structure, or into an amorphous state. On the other hand the complexity of the crystalline structure does not affect the likelihood to crystallize. In particular, our giant unit cell crystals are readily formed in Monte-Carlo simulations of large systems.

Perhaps the most telling conclusion from this study comes from a negative result. Despite our comprehensive inclusion of all possible local structures, we never found a local structure so geometrically 'awkward' that it lacked a crystalline groundstate: our enumerative procedure to find crystalline structures always provided the lower bound on observed energies. Furthermore, every choice of FLS (with a single exception), exhibited a relatively rapid crystallization, if not always to the ground state. While the choice of FLS can influence the size of the unit cell in the crystal and the degree of ordering in the supercooled liquid, we conclude that the existence and kinetic accessibility of the crystalline phase are essentially independent of the nature of the local structure. As for the liquid state, it is clearly the multiplicity of the FLS, not its geometrical structure, that exerts the most important influence with regards the accumulation of structure in the liquid and any associated slowing down. This conclusion challenges the long lived tradition of assigning significance to the presence of specific local structures in low temperature liquids.

Acknowledgements

We thank Sinai Robins for pointing out the correspondence between Hermite matrices and crystalline structures on a lattice. We thank Hanna Grönqvist for useful comments. PH acknowledges the financial support of the Australian Research Council and PR acknowledges the hospitality of the School of Chemistry at the University of Sydney where this work was initiated. Three dimensional pictures were realized with Mayavi [28], plots with Matplotlib [29].

[1] C. P. Royall and S. R. Williams, *Phys. Rep.* **560** (2015).
 [2] Y.Q.Cheng and E. Ma, *Prog. Mater. Sci.* **56**, 379 (2011).
 [3] F. C. Frank, *Proc. Royal Soc (London) A*, **215**, 43

(1952).
 [4] G. Tarjus *et al.*, *J. Phys.: Condens. Matter*, **17** R1143 (2005).

- [5] P. Ronceray and P. Harrowell, *J. Chem. Phys.* **136**, 134504 (2012).
- [6] U. R. Pedersen, T. B. Schroder, J. C. Dyre, and P. Harrowell, *Phys. Rev. Lett.* **104**, 105701 (2010).
- [7] P. Ronceray and P. Harrowell, *Europhys. Lett.* **96**, 30065 (2011).
- [8] P. Ronceray and P. Harrowell, *Phys. Rev. E.* **87**, 052313 (2013).
- [9] P. Ronceray and P. Harrowell, *Phys. Rev. Lett.* **112**, 017801 (2014).
- [10] See Supplementary Material available for download at <http://sjscience.org/article?id=77> for details on the groundstate structures, energies and phase transition behaviour for each choice of the Favoured Local Structure.
- [11] J. K. Kummerfeld, T. S. Hudson, and P. Harrowell, *J. Phys. Chem. B* **112**, 10773 (2008); L. Filion and M. Dijkstra, *Phys. Rev. E* **79**, 046714 (2009). (2009); A. B. Hopkins, Y. Jiao, F. H. Stillinger and S. Torquato, *Phys. Rev. Lett.* **107**, 125501 (2011).
- [12] M. P. Tosi, *J. Mol. Liquids* **83**, 23 (1999).
- [13] T. Uchino, *J. Ceramic Soc. (Japan)* **1313**, 17 (2005).
- [14] A. B. Bortz, M. H. Kalos and J. L. Lebowitz, *J. Comp. Phys.* **17**, 10 (1975).
- [15] G. Hart and R. Forcade, *Phys. Rev. B* **77**, 224115 (2008).
- [16] J. A. van Meel, B. Charbonneau, A. Fortini and P. Charbonneau, *Phys. Rev. E* **80**, 061110 (2009).
- [17] E. R. Chen, D. Klotsa, M. Engel, P. F. Damasceno and S. C. Glotzer, *Phys. Rev. X*, **4**, 011024 (2014).
- [18] J. de Graaf, R. van Roij, and M. Dijkstra, *Phys. Rev. Lett.* **107**, 155501 (2011)
- [19] L. Pasteur, *Comptes rendus de l'Académie des Sciences (Paris)*, **26**, 535 (1848).
- [20] J. Jacques, A. Collet, and S. H. Willen, *Enantiomers, Racemates, and Resolutions* (Wiley, New York, 1981).
- [21] L. Pauling, *Am. Sci.* **43**, 285 (1955).
- [22] K. Urban and M. Feuerbacher, *J. Non-Cryst. Sol.* **334 - 335**, 143 (2004).
- [23] W. Kauzmann, *Chemical Reviews* **43**, 219 (1948).
- [24] C. A. Angel, in *Structural Glasses and Supercooled Liquids: Theory, Experiment, and Applications*, ed. P. G. Wolynes and V. Lubchenko (Wiley, New York, 2012), pp. 241-2.
- [25] M. B. Thompson, arXiv:1011:0175 (2010).
- [26] L. Yu, *Accounts Chem. Res.* **43**, 1257 (2010).
- [27] R. Brand, P. Lunkenheimer and A. Loidl, *J. Chem. Phys.* **116**, 10386 (2002).
- [28] P. Ramachandran and G. Varoquaux, *Comput. Sci. Eng.* **13**, 40 (2011).
- [29] J. D. Hunter, *Comput. Sci. Eng.*, **9** (3), 90-95 (2007).
- [30] The number in parentheses correspond to the standard deviation of the distribution, over the considered set of FLS.

Appendix A: Enumerative method for determining ground states

Our method for determining ground state structures and energies makes use of a correspondence between crystalline base vectors on a lattice and number-theoretical objects called Hermite matrices. A similar approach was introduced by Hart and Forcade [15] as a tool to study derivative structures for metallic alloys. The idea is to list all possible sets of crystalline base vectors (superlattice) on the FCC lattice. There are 17602 distinct superlattices of the FCC lattice with up to $Z = 80$ sites per crystalline cell (having eliminated redundancies due to reparametrization and lattice symmetries). We use the correspondence between superlattices and integer matrices in the Hermite normal form, completed by a reduction using the FCC symmetries, to obtain this set of structures. For each such superlattice and every FLS, we find the best crystalline spin configuration associated to this superlattice by simulated annealing of the spin variables of a single crystal cell, with appropriate boundary conditions. The small number of spins involved in this makes us confident that the best spin structure is found. Whenever necessary, we extend this procedure up to 128 sites per cell. This systematic approach is complemented with a more standard Monte-Carlo simulated annealing using a rejection-free algorithm [14] of a large system of up to 24^3 sites, which always gives a resulting minimal energy higher or equal to that obtained in the enumerative procedure. While these approaches can in principle fail and fall in metastable minima, we are confident that most (if not all) of the ground states are indeed the global ones.